organoids

MDPI

Article

Heparin-Binding Epidermal-like Growth Factor (HB-EGF) Reduces Cell Death in an Organoid Model of Retinal Damage

Michelle N. H. Tang [1], Mariya Moosajee [1], Najam A. Sharif [2], G. Astrid Limb [1] and Karen Eastlake [1,2,*]

[1] NIHR Biomedical Research Centre at Moorfields Eye Hospital and UCL Institute of Ophthalmology, London EC1V 9EL, UK; michelle.tang@alumni.ucl.ac.uk (M.N.H.T.); g.limb@ucl.ac.uk (G.A.L.)
[2] Department of Global Alliances and Collaboration, Global Ophthalmology Research & Development, Santen Incorporated, Emeryville, CA 94608, USA; nsharif@nanostherapeutics.com
* Correspondence: k.eastlake@ucl.ac.uk

Abstract: In zebrafish and various mammalian species, HB-EGF has been shown to promote Müller glia proliferation and activation of repair mechanisms that have not been fully investigated in human retina. In the current study, 70- to 90-day-old human retinal organoids were treated with 20 µM 4-hydroxytamoxifen (4-OHT), and CRX, REC, NRL, PAX6, VIM, GFAP, and VSX2 gene and protein expression were assessed at various times points after treatment. Organoids with or without 4-OHT-induced damage were then cultured with HB-EGF for 7 days. We showed that 20 µM 4-OHT caused a reduction in the number of recoverin-positive cells; an increase in the number of TUNEL-positive cells; and downregulation of the photoreceptor gene markers CRX, NRL, and REC. Culture of organoids with HB-EGF for 7 days after 4-OHT-induced damage caused a marked reduction in the number of TUNEL-positive cells and small increases in the number of Ki67-positive cells and PAX6 and NOTCH1 gene expression. The current results suggest that treatment of human ESC-derived retinal organoids with 4-OHT may be used as a model of retinal degeneration in vitro. Furthermore, HB-EGF treatment of human retinal organoids increases proliferating Müller cells, but only after 4-OHT induced damage, and may be an indication of Muller reactivity in response to photoreceptor damage. Further studies will aim to identify factors that may induce Müller cell-mediated regeneration of the human retina, aiding in the development of therapies for retinal degeneration.

Keywords: Müller glia; retina; stem cells; retinal organoids; photoreceptors; degeneration; endogenous regeneration

Citation: Tang, M.N.H.; Moosajee, M.; Sharif, N.A.; Limb, G.A.; Eastlake, K. Heparin-Binding Epidermal-like Growth Factor (HB-EGF) Reduces Cell Death in an Organoid Model of Retinal Damage. *Organoids* **2024**, *3*, 148–164. https://doi.org/10.3390/organoids3030010

Academic Editors: James Adjaye and Nina Graffmann

Received: 30 May 2024
Revised: 27 June 2024
Accepted: 3 July 2024
Published: 5 July 2024

1. Introduction

Retinal degenerative conditions, such as age-related macular degeneration (AMD), diabetes, and retinitis pigmentosa, are characterized by progressive neural cell loss that ultimately leads to blindness. As current treatments may slow the progression of the disease but do not reverse the damage, patients can still experience visual decline. There is therefore a need for novel therapies to protect, repair, or restore damaged retinal cells in situ. Our previous research on human Müller glia have suggested that they might constitute a tool to explore the potential for endogenous cellular regeneration [1,2]. However, there is currently a lack of in vitro models of human retinal degeneration to study novel approaches for retinal repair. The development of such in vitro models could facilitate the investigation of novel repair mechanisms, while reducing the use of animal models that do not fully resemble human disease.

Müller glia are the principal glial cells of the retina that provide homeostatic and structural support to all retinal neurons [3]. These cells have the ability to regenerate the retina in some species such as *Xenopus* and zebrafish [4,5]. A limited retinal regenerative response has also been identified in chick and rodent retina [6,7]. Although previous studies have identified a population of Müller glia with neural stem cell characteristics in the human

retina [8,9], currently there is no evidence for spontaneous regeneration. Transplantation studies using a human Müller cell line (MIO-M1 cells) and Müller cells isolated from retinal organoids derived from human iPSCs have shown improvements in visual function in rodent models of retinal degeneration [2,10] without evidence of integration into the retina, suggesting that some of the therapeutic benefit arises through paracrine signaling. Although cell transplantation as a treatment for retinal diseases provides some advantages, such as personalized medicine and autologous transplantation, it requires vast resources, invasive procedures, and complex treatments for patients, such as immunosuppression. Therefore, approaches to induce self-repair of the retina by injection of therapeutic agents would be preferable. Recent studies in both zebrafish and mammals have tried to unlock the regenerative potential of mammalian Müller glia through the exploration of molecular mechanisms of neurogenesis induced by these cells [11–14].

HB-EGF activates the epidermal growth factor (EGF) signaling pathway and has high affinity for the EGF receptor (EGFR) [15]. In the zebrafish retina, activation of EGFR via HB-EGF results in the dedifferentiation and proliferation of Müller glia, triggered by activation of HB-EGF/EGFR/MAPK signaling. This process has been shown to be necessary and sufficient for Müller glia-mediated regeneration in this species [16]. More recent studies have investigated the effect of HB-EGF in mammalian retina and have shown that this factor can stimulate Müller glia proliferation in damaged rodent retina by activating MAPK signaling as well as mTOR and Jak/Stat signaling [17]. It has also been shown that the HB-EGF/Ascl1/Lin28a pathway is activated in Müller cells obtained from adult rats after exposure to retinal pigment epithelium (RPE) supernatant treated with PNU-282987, a nicotinic acetylcholine receptor agonist that acts on RPE to stimulate production of Müller-derived progenitor cells [12]. In addition, HB-EGF is upregulated in human retinae during proliferative vitreoretinopathy (PVR) and increases the in vitro proliferation of the human Müller cell line MIO-M1 [18]. Since experiments in zebrafish and rodent retinae cannot be replicated in humans, the use of human stem cell-derived retinal organoids constitutes an ideal platform to investigate mechanisms of human retinal degeneration and novel methods to induce the regeneration of the human retina.

Photoreceptor degeneration in mice retinal explants [19] or mouse induced pluripotent stem cell (iPSC)-derived retinal organoids [20] can be induced using 4-hydroxytamoxifen, an inverse agonist of the orphan nuclear hormone receptor estrogen-related receptor β (ERRβ). Using published protocols of organoid damage in other species [20], this study aimed to investigate whether HB-EGF may exert regenerative-like effects in human embryonic stem cell (ESC)-derived retinal organoids after induction of photoreceptor cell death. The results confirm that treatment of human ESC-derived retinal organoids with 4-OHT might be a used as a model of retinal degeneration in vitro and that 7-day treatment of damaged organoids with HB-EGF leads to an increase in proliferating Müller cells. Although there was no evidence of regeneration of photoreceptor-like cells in these organoids, we hypothesize that Müller cell proliferation may indicate initiation of reactivity within the organoid. Further long-term studies will aim to identify mechanisms that may induce Müller cell-mediated regeneration of the human retina, which may aid in the future development of retinal regenerative therapies.

2. Materials and Methods

2.1. Stem Cell Cultures and Retinal Organoid Differentiation

Human embryonic stem cells (RC9 cells Research Grade, Roslin cells/UK Stem Cell Bank [21]) were maintained in Stem-Pro complete medium (A1000701; Thermo Fisher Scientific, Horsham, UK) containing 1% 100× penicillin/streptomycin and grown on plates coated with 0.05 mg/mL human Vitronectin (A14700; Thermo Fisher Scientific). Differentiation of human pluripotent stem cells into retinal organoids was based on previously published protocols [2]. Briefly, upon 80% confluency, cells were washed with 1× phosphate-buffered saline (PBS), detached with TryplE (Thermo Fisher) containing 10 µM ROCKi (Y-27632, Millipore, Watford, UK) and 0.5 mg/mL DNase (Sigma-Aldrich,

Haverhill, UK), and pelleted. Cells were seeded at a density of 9000 cells per well in a v-bottomed 96-well plate (PrimeSurface Sumilon low adhesion, Alpha Laboratories, Eastleigh, UK) in Glasgow Minimum Essential Medium (GMEM) with l-glutamine containing 20% KOSR (KnockOut serum replacement; Thermo Fisher), 1% 100× sodium pyruvate (Thermo Fisher, Horsham, UK), 1% 100× nonessential amino acids (Thermo Fisher), 1% 100× penicillin/streptomycin (Thermo Fisher, Horsham, UK), and 50 μM β-mercaptoethanol. The media was supplemented with 20 μM ROCKi and 3 μM Wnt antagonist as indicated (Millipore, Watford, UK). On days 2, 5, and 9, 100 μL of the same media supplemented with 20 μM ROCKi, 3 μM Wnt antagonist, and a final concentration of 1% Matrigel was placed in the wells. On day 12, the embryoid bodies (EBs) that formed were transferred into separate wells of a 25-well squared, low-adhesion plate and incubated in the above media (without ROCKi and WNT antagonist) with the addition of 10% FBS, 1% Matrigel, and 100 nM smoothened agonist (SAG; Millipore, Watford, UK). On day 15, the medium was replaced. On day 18, the medium was replaced with Dulbecco's modified Eagle's medium/F12-glutamax containing 10% FCS, 1% 100× N2 supplement (Thermo Fisher, Horsham, UK), 1% penicillin/streptomycin/amphotericin, and 0.5 μM retinoic acid (Sigma-Aldrich, Haverhill UK). Retinal organoids were then fed twice weekly with the above media for study duration. From days 30 to 50, retinal organoids were dissected under the microscope using microblades and placed into new 25 square low-adhesion plates to ensure that only neural retinal tissue remained and matured in culture. All cells and organoids were maintained at 37 °C, 5% CO_2, and atmospheric O_2.

2.2. 4-OHT and HB-EGF Treatment of Retinal Organoids

Using published protocols by others, see Refs. [20,22], human retinal organoids between 70 and 90 days were cultured in the presence or absence of 4-OHT (5 μM, 10 μM, 20 μM, or 50 μM) in DMEM F12 supplemented with 10% KOSR for up to 7 days. At least three replicates were performed consisting of different organoid 'batches' where the cultures were initiated on differing days. Retinal organoids were collected at 24 h, 3 days, or 7 days to assess photoreceptor and Muller glia marker expression using immunofluorescence staining and qPCR. At least 3 organoids were collected for histological analysis per replicate and at least 4 organoids were pooled per replicate to isolate enough RNA for gene analysis using qPCR.

For HB-EGF treatment, retinal organoids aged between 70 and 90 days were first subject to incubation with 20 μM 4-OHT in DMEM F12 containing 10% KOSR for 24 h. Retinal organoids were then washed three times in DMEM F12 supplemented with 10% KOSR prior to the addition of 1 mL of 100 ng/mL HB-EGF in DMEM F12 supplemented with 10% KOSR per organoid. At least three replicates were performed consisting of different organoid 'batches' where the cultures were initiated on differing days. Samples of retinal organoid tissue were collected at 7 days to assess photoreceptor marker expression using histology and qPCR. At least 3 organoids were collected for histological analysis per replicate, and at least 4 organoids were pooled per replicate to isolate enough RNA for gene analysis by qPCR.

2.3. Immunofluorescence and Cell Analysis

Retinal organoids were rinsed in PBS before fixation in 4% paraformaldehyde overnight at 4 °C. On the following day, a half volume of 30% sucrose was added to the organoids in fixative to create a 1:1 mix and left overnight. This was then replaced with total 30% sucrose overnight at 4 °C. Organoids were then embedded in OCT compound, snap frozen using acetone and dry ice, and sectioned to 12 μm using a Leica Cryostat (Leica Microsystems Ltd., Milton Keynes, UK). Slides were blocked for 1 h in TBS + 0.3% triton + 5% donkey serum before the addition of the primary antibody (diluted in blocking buffer). Primary antibodies (see Supporting Information Table S1) were incubated overnight at 4 °C, followed by three washes with TBS for 5 minutes each. Secondary antibodies (Alexa Fluor, Invitrogen, Cheshire, UK, 1:500 in TBS + 0.3% triton) were incubated for 3 h at room

temperature in the dark. Slides were then washed in TBS, mounted with Fluoroshield Mounting Medium containing 4′,6-diamidino-2-phenylindole (DAPI; Abcam, Cambridge, UK), coverslipped, and sealed with nail varnish.

2.4. Image Analyses

ImageJ (ImageJ 1.51j8; http://imagej.nih.gov/ij (accessed on 29 May 2024)) was used to perform cell counts with manual counting. Alternatively, ImageJ was used to invert the color and convert images to 8-bit greyscale prior to applying binary watershed and performing the 'analyze particles' command using a particle cut-off with an area < 500 pixels. Selected image counts were verified with manual counting. For each replicate, at least 3 images were taken for cell count analyses. Graphs were generated and statistical analyses were performed using GraphPad Prism software (Graphpad Prism 8.0) using one-way ANOVA (Bonferroni post hoc test) or Student's *t* test. Data sets were plotted as mean ± SEM, and results were considered significant for $p < 0.05$.

Fluorescence intensity was measured using ImageJ by selecting regions of interest (retinal organoid section) and measuring the integrated density (sum of the pixel intensity over all of the pixels in an object) of the selected fluorophores. Background intensity (averaged from ×10 images) was subtracted from the measured signal. Therefore, the corrected fluorescence intensity = integrated density − (selected area × background fluorescence).

2.5. Reverse Transcription and Quantitative PCR

Total RNA was isolated using Qiagen Rneasy Micro Plus kits (Qiagen, Manchester, UK) according to manufacturers' protocols. SuperScript® IV First-Strand Synthesis System (Life Technologies, Horsham, UK) was used to perform reverse transcription per the manufacturer's instructions. Briefly, 100–500 ng RNA was added to a mix of 0.5 µg oligo (dT) 12–18 primers (Life Technologies) and 0.5 mM dNTPs (Life Technologies) and heated to 65 °C for 5 min using an Eppendorf Mastercycler (Eppendorf, Stevenage, UK). Then, 5 mM DTT, 40 U of RNasin Plus (Promega, Chilworth, UK), and 200 U of Superscript IV in first strand buffer was then added to the reaction mix and further incubated at 55 °C for 10 min. Then, the sample was heated to 80 °C for 10 min to generate cDNA. cDNA was stored at −20 °C.

The qRT-PCR was performed using Luna® Universal qPCR Master Mix (New England Biolabs, Hitchin, UK) following protocols from the manufacturer. Predesigned KiCqStart® SYBR® Green Primers were used for selected genes including CRX, REC, NRL, PAX6, and NOTCH1 (Sigma-Aldrich, See Supporting Information Table S2). The following thermocycling conditions were used: 95 °C for 10 min followed by 40 cycles of 95 °C for 15 s and 60 °C for 1 min. The data were analyzed using the $2^{-\Delta\Delta Ct}$ method as fold change relative to GAPDH and 18S as endogenous controls. All samples were run in triplicate. All graphs are expressed as log2-fold change as compared to untreated controls.

3. Results

3.1. 4-OHT Dose Response and Changes in Retinal Morphology

To induce moderate photoreceptor damage in human ESC-derived retinal organoids, we cultured organoids for up to 7 days in a range of 4-OHT concentrations (10 µM, 20 µM, or 50 µM). The current experiments used 70- to 90-day-old organoids, reflecting a stage of maturation where photoreceptors express robust recoverin expression [22]. We assessed the resulting pathology based on organoid morphology, retinal section thickness, and quantification of TUNEL-positive staining. Treatment with different concentrations of 4-OHT for 24 h caused changes in organoid morphology, characterized by reduction in growth and loss of retinal structures as compared to controls. Specifically, 50 µM 4OHT induced complete loss of retinal organoid structure, as shown by loss of transparency in the outer lobes of the organoid observed in phase contract images after 24 h (Figure 1A, bottom panel, blue arrows). Further analysis of organoids cultured with 50 µM 4-OHT was not possible due to the fragility of the tissue. In all other conditions, there was no clear

differences in the phase contrast images of the retinal organoids (Figure 1A). Representative confocal images show that TUNEL-positive cells (green) are visibly increased upon the addition of 10 μM 4-OHT; however, there were no observable differences over 24 h, 3 days, and 7 days (Figure 1B). The addition of 20 μM 4-OHT showed more pronounced increases in the number of TUNEL-positive cells, which were observed throughout the whole width of the retinal organoid. The number of TUNEL-positive cells was observed to increase over 7 days for organoids incubated with 20 μM 4-OHT but not 10 μM 4-OHT (Figure 1B). Retinal thickness was analyzed by measuring the cell layers from the RGC-like layer to the outer photoreceptor layer using immunofluorescent images obtained under confocal microscopy (White arrows, Figure 1B). There was a trend in the reduction in retinal organoid thickness in those treated with 20 μM 4-OHT over time; however, only those treated with 20 μM 4-OHT for 7 days were shown to be significantly thinner as compared to controls (Figure 1C, $p < 0.001$). There was no significant difference in retinal thickness in organoids treated with 10 μM 4-OHT at all time points tested. Analysis of apoptotic cells with immunofluorescence staining showed a significant increase in the percentage of TUNEL-positive cells when organoids were incubated with 10 μM and 20 μM 4-OHT for 24 h, 3 days, and 7 days as compared to controls (Figure 1D). However, addition of 10 μM 4-OHT did not cause any observable microscopic retinal organoid damage or increase in cell death. On this basis, subsequent experiments were performed using 20 μM 4-OHT to induce moderate damage in the retinal organoids.

3.2. Confirmation of Photoreceptor Degeneration Induced by 20 μM 4-OHT

Based on the initial results, we further explored the effect of 20 μM 4-OHT on the photoreceptor and Müller cell populations of retinal organoids over a 7-day period. Immunostaining of retinal organoids for expression of recoverin, a photoreceptor marker, showed a developing photoreceptor layer, with recoverin-positive cells located on the outer edge at the top of the confocal image cross-sections (Figure 2A). Recoverin-positive staining was also observed in the inner layers of the retinal organoids (located towards the bottom of the images) and might therefore be indicative of a bipolar cell type that also expresses this marker. Examination of cell morphology and distribution within the organoid after the addition of 20 μM 4-OHT showed that recoverin-positive cells gradually lost their characteristic morphology and became rounded as incubation progressed from 24 h to 7 days (white arrows, Figure 2A). Quantification of recoverin-positive photoreceptors showed a significant decrease in cell number per mm^2 of retina at 24 h and 7 days (Figure 2B). Cell death, as assessed using TUNEL staining, showed a gradual increase in the number of positive cells as the time of incubation with 4-OHT progressed, which can be clearly observed in Figure 2A. There was a significant increase in the percentage of TUNEL-positive cells as compared to control at all time points examined (as previously shown in Figure 1D). Assessment of the expression of photoreceptor-related gene markers using qPCR showed that after 24 h of incubation with 20 μM 4-OHT, there was a marked log2-fold decrease in NRL expression and slight increases in CRX and REC expression, as compared to controls. A marked fold reduction in the expression of CRX, NRL and REC was observed after 3 days incubation with 20 μM 4-OHT, and this was maintained for 7 days (Figure 2C).

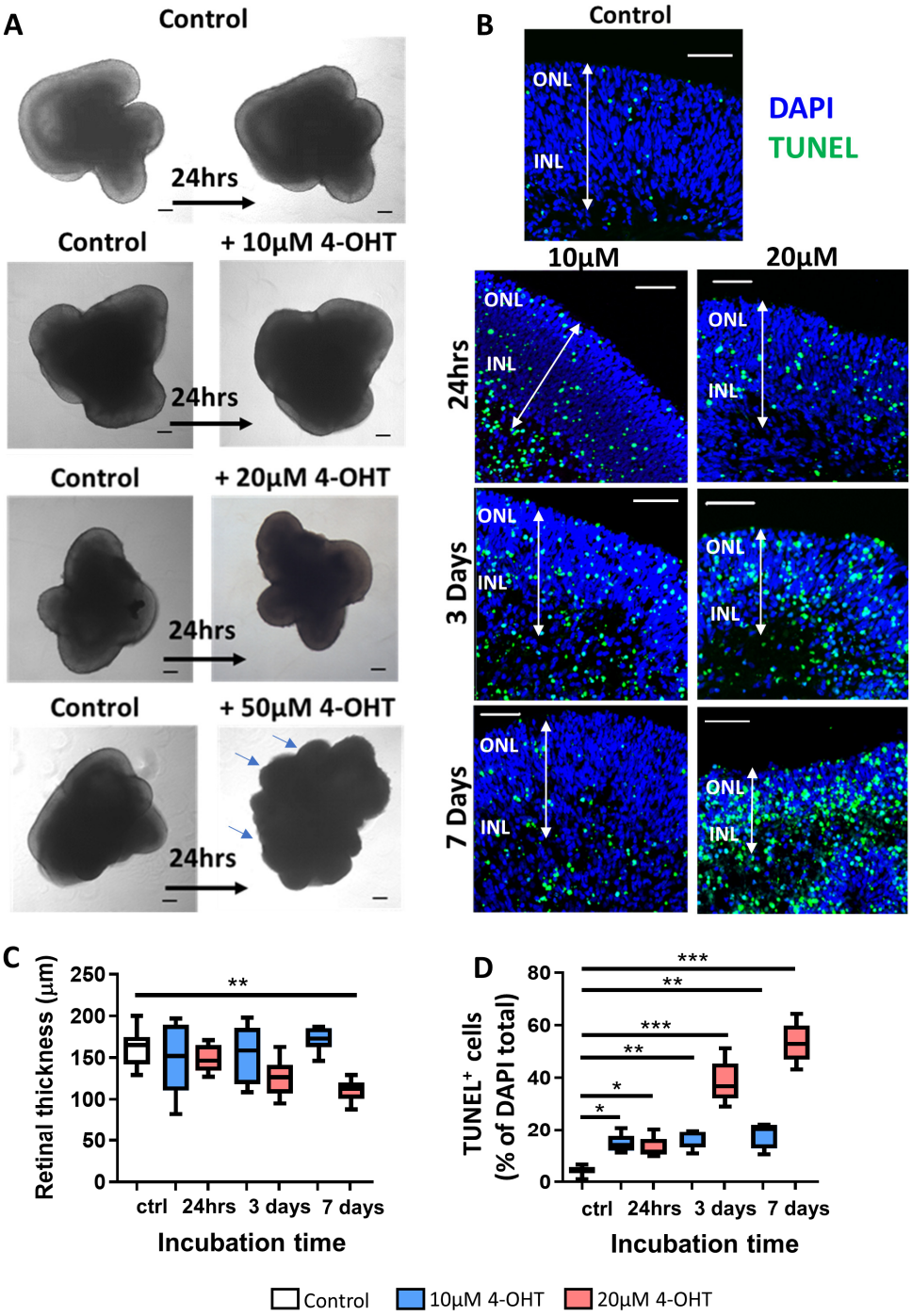

Figure 1. Morphological changes induced by 4-OHT in retinal organoids. (**A**) Phase contrast images of retinal organoids after 24 h treatment (black arrows) with or without the addition of different 4-OHT concentrations (10, 20, or 50 µM). Scale 200 µm. (blue arrows show bulging and loss of transparency) (**B**) Representative confocal images of retinal organoid cross-sections showing TUNEL-positive nuclei (green) and counterstained with DAPI (blue) to indicate total cell nuclei. Scale 50 µm. ONL = outer nuclear layer; INL = inner nuclear layer. (**C**) Box plot shows the average thickness (µm) of retinal layers in organoids after treatment with or without 4-OHT (10 or 20 µM) over a 7-day period (n = 6). (**D**) Box plot shows the percentage of TUNEL-positive cells in retinal organoids treated with 4-OHT (10 or 20 µM) as compared to those without treatment (control) over 7 days (n = 3). * $p < 0.05$; ** $p < 0.01$; *** $p < 0.001$; Student's t test. One-way ANOVA. Error bars represent SEM.

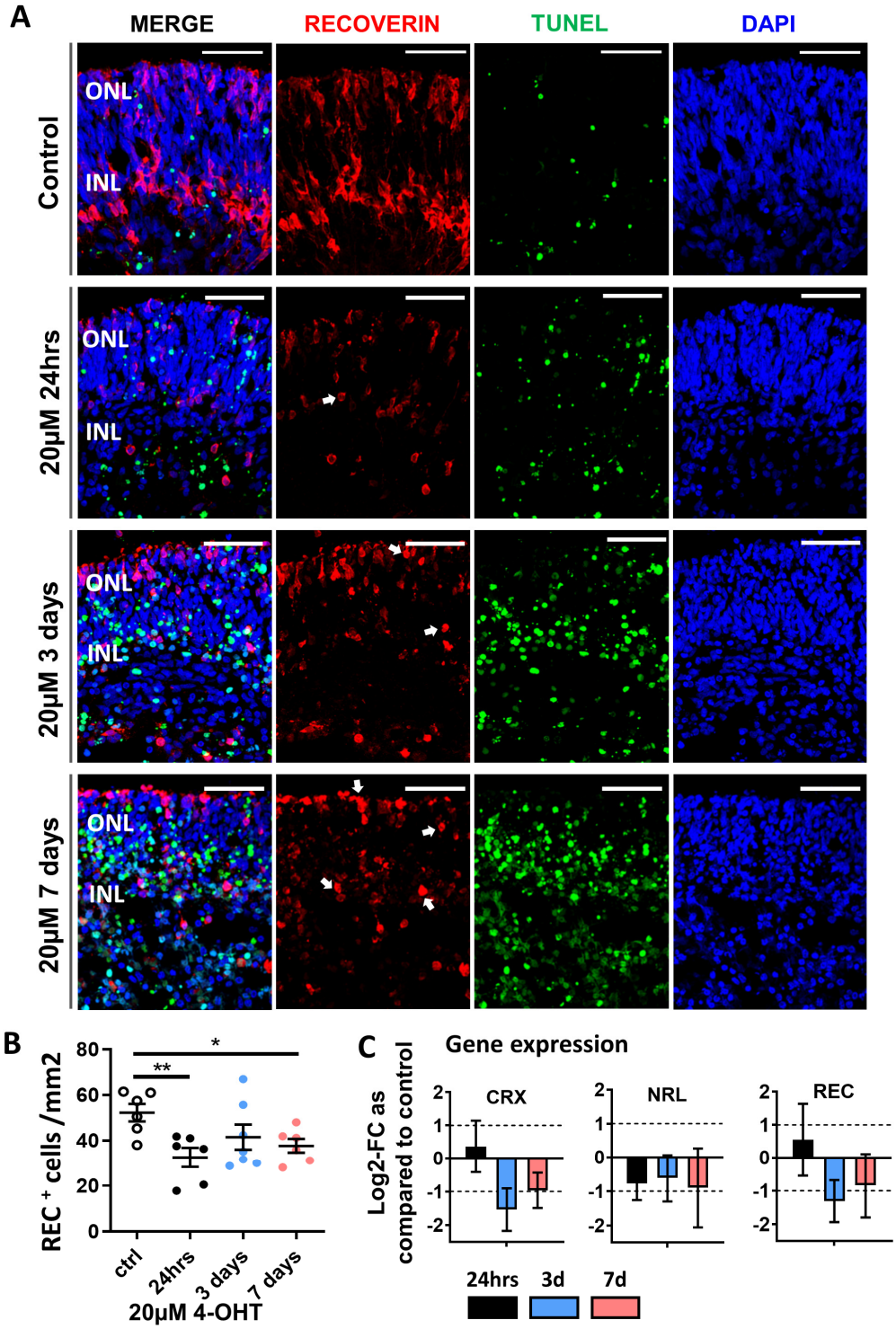

Figure 2. Photoreceptor degeneration induced by 4-OHT. (**A**) Representative confocal images of control retinal organoids and retinal organoids after 20 µM 4-OHT treatment for 24 h, 3 days, and 7 days. Sections show expression of recoverin (red) and cell death observed with TUNEL (green) staining. Cell nuclei were detected with DAPI (blue). (White arrows show rounded cells after damage) 40× magnification; scale 50 µm. ONL = outer nuclear layer; INL = inner nuclear layer. (**B**) Scatter plot shows the number of recoverin-positive cells (per mm^2) in retinal organoids treated with 4-OHT (20 µM) as compared to those without treatment (control) at each time point (24 h, 3 days, 7 days). $n = 3$; (each n represents 3 images). (**C**) Graphs show the relative log2-fold change (FC) in expression of the photoreceptor-related genes CRX, NRL, and REC after 4-OHT treatment for 24 h, 3 days, or 7 days as compared to untreated control organoids. * $p < 0.05$; ** $p < 0.01$; $n = 4$. Error bars represent SEM.

3.3. Müller Glia Responses to 4-OHT Treatment of Retinal Organoids

Little is known about the responses of Müller glia to damage induced in human ESC-derived retinal organoids. We therefore examined the responses of these cells to the optimized concentration of 20 μM 4-OHT over time. Gradual loss of retinal structure, including rounder cell nuclei and fragmentation of Müller cell processes, was observed, increasing from days 3 to 7, as seen by the microscopical examination of organoids stained for the classical Müller cell marker vimentin (Figure 3A). Confocal examination of immunofluorescence staining indicated that the number of cells expressing the proliferation marker Ki67 slightly increased at 7 days with 4-OHT treatment; however, this was not statistically significant (Figure 3A,B). There was, however, a significant decrease in the number of cells positive for VSX2 (Chx10, expressed by progenitors and Müller cells) per mm^2 of retina after 7-day incubation with 20 μM 4-OHT as compared to control (Figure 3A,C). Examination of the cells that were double positive for both Ki67 and VSX2 did not show any significant changes (Figure 3D). We sought to examine whether there was any reactivity of the Muller glia cells with the examination of GFAP levels within the cells and the levels of SOX2, a neural progenitor marker, known to be expressed in retinal progenitor cells, a subpopulation of Muller glia with progenitor characteristics. The patterns of SOX2-expressing cells showed that these cells were located in the middle layers of the retinal organoids, and the numbers appeared to be consistent among all 4-OHT concentrations tested (Figure 3E). Expression of GFAP, a marker of activated Müller cells during gliosis, co-localized with vimentin as expected, and visible increases in fluorescence intensity were noted after 24 h and 3 days of organoid treatment with 20 μM 4-OHT (Figure 3E). To confirm changes in expression of GFAP upon 4-OHT treatment, we examined the fluorescence intensity of the confocal images, which showed a significant increase at 24 h only as compared to controls (Figure 3F). Whilst the intensity of GFAP intensity appeared to decrease after 7 days of 4-OHT incubation, the morphology of the cell processes as shown by vimentin and GFAP immunofluorescence appears disrupted and less regular than that of controls or those at 24 h or 3 days of treatment with 20 μM 4-OHT, suggesting that Muller glia may be negatively affected by a long-term 4-OHT insult (Figure 3E). A decrease in GFAP gene expression was observed after 24 h and 7 days compared to control organoids as determined using qPCR, whereas a slight increase in the log2-fold change of expression as compared to control (day 0) was seen at 3 days (Figure 3G). We therefore concluded that treatment with 4-OHT for 24 h was sufficient to cause developing photoreceptor degeneration and trigger an acute Muller glia response mediated by the upregulation of GFAP. The following experiments were therefore conducted by inducing damage with 20 μM 4-OHT for 24 h prior to addition of HB-EGF for an additional 7 days.

3.4. Partial Restoration of Retinal Organoid Morphology upon Incubation of 4-OHT-Damaged Organoids with HB-EGF

After establishing the damage induced by 20 μM 4-OHT in this model of retinal degeneration in vitro, we subsequently investigated whether HB-EGF exhibited protective and regenerative effects on retinal organoids after induced degeneration. Following the induction of acute damage to human retinal organoids with 20 μM 4-OHT for 24 h, 100 ng/mL HB-EGF was added to the organoid culture medium and incubated for an additional 7 days and compared to those without HB-EGF treatment. Histological examination of retinal organoid morphology showed no obvious changes when retinal organoids were incubated with 100 ng/mL HB-EGF alone for 7 days (Figure 4A). However, 20 μM 4-OHT treatment for 24 h followed by the addition of medium alone for 7 days resulted in cell death and marked retinal degeneration as indicated by the distribution of rounder and fragmented nuclei (stained with DAPI) (Figure 4A). When retinal organoids were treated with HB-EGF for 7 days after 24 h incubation with 4-OHT, retinal organoid morphology and cellular organization appeared to be partially restored as indicated by the lack of nuclei fragmentation (DAPI staining) and characteristic cellular staining for recoverin (Figure 4A). Furthermore, there were fewer rounded recoverin-positive cells observed in organoids treated with

HB-EGF as compared to those treated with 4-OHT alone (Figure 4A, also see Figure 2A, arrows). Examination of apoptosis using TUNEL staining showed a significant increase in the percentage of positive cells (of DAPI total) when organoids were treated with 20 µM 4-OHT followed by 7 days of incubation in medium alone (Figure 4A,B). Furthermore, it was noted that when organoids were treated with 4-OHT and HB-EGF, the percentage of TUNEL-positive cells was significantly lower than organoids treated with 4-OHT alone (Figure 4B), indicating that HB-EGF had reduced cell death. Treatment of retinal organoids with 4-OHT followed by the addition of medium alone showed a significantly lower number of recoverin-positive cells (per mm^2 of retina) as compared to control after 7 days (Figure 4B). Whilst small increases were observed in the number of recoverin-positive cells (per mm^2) when organoids were incubated with HB-EGF after 4-OHT treatment, these did not reach statistical significance (Figure 4B). Retinal thickness measurements were also examined. Although no differences were observed between controls or organoids treated with HB-EGF only or 4-OHT alone, there was a significant increase in retinal organoid thickness when treated with 4-OHT and HB-EGF as compared to those treated with 4-OHT alone (Figure 4C).

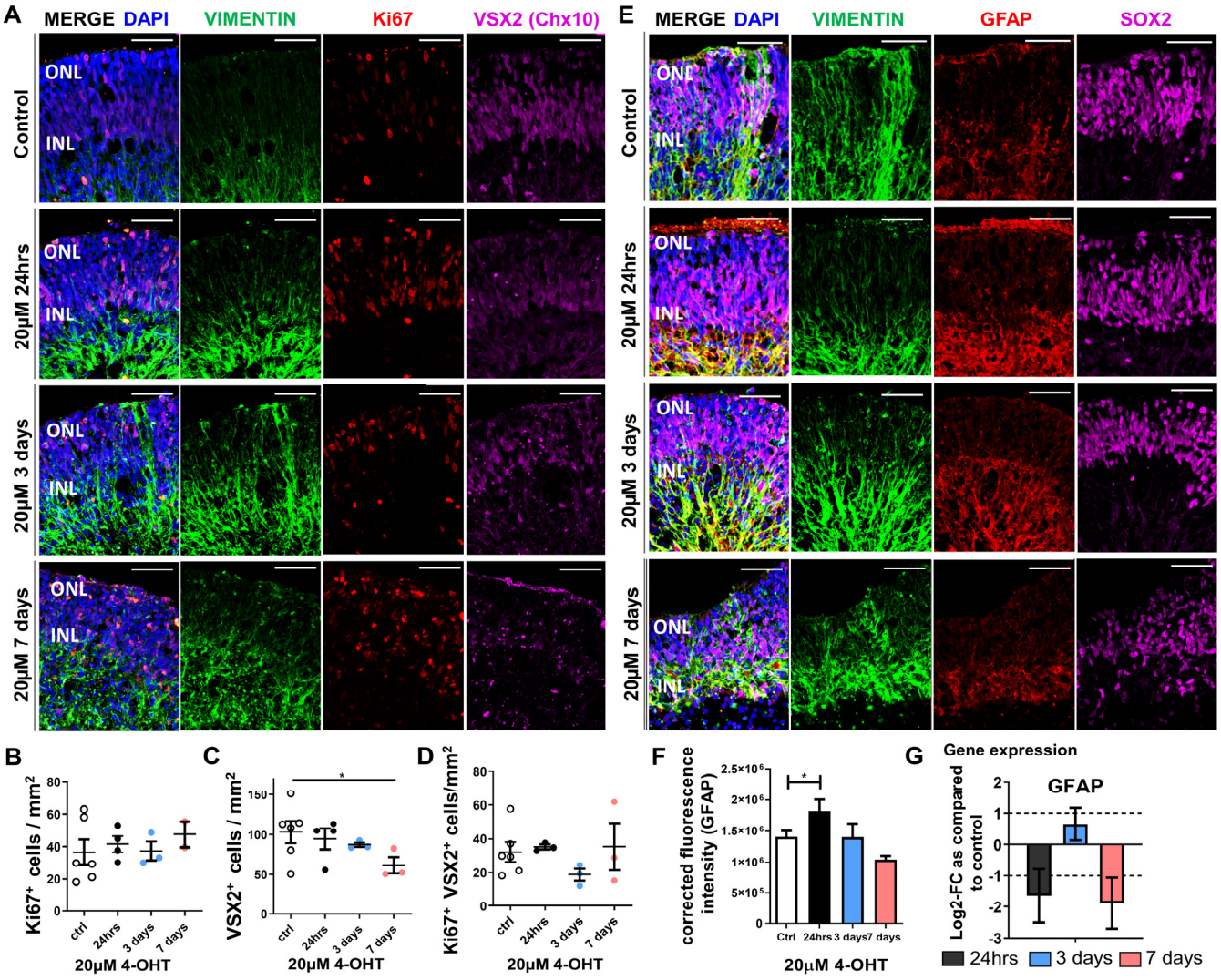

Figure 3. Müller cell responses to 4-OHT treatment. (**A**,**E**) Representative confocal images of retinal organoids after 20 µM 4-OHT treatment for 24 h, 3 days, and 7 days. Sections show expression of (**A**) vimentin (green), Ki67 (red), and VSX2 (magenta) as well as (**E**) vimentin (green), GFAP (red), and

SOX2 (magenta). Cell nuclei were detected with DAPI (blue). 40× magnification; scale 50 µm. ONL = outer nuclear layer; INL = inner nuclear layer. (**B**–**D**) Dot plot shows the proportion of cells positive for Ki67 (**B**) and VSX2 (Chx10) (**C**) (per mm^2) and those that were double positive for Ki67 and VSX2 (per mm^2) (**D**) in retinal organoids treated with 4-OHT (20 µM) as compared to those without treatment (control) at each time point (24 h, 3 days, and 7 days). (**F**) Bar graphs show the measured intensity of GFAP staining from confocal images using ImageJ analysis and (**G**) the relative log2-fold change (FC) in expression of the Müller cell gliosis related gene GFAP after 4-OHT treatment for 24 h, 3 days, or 7 days as compared to untreated control organoids. $n = 4$; * $p < 0.05$. Student's *t* test; one-way ANOVA.

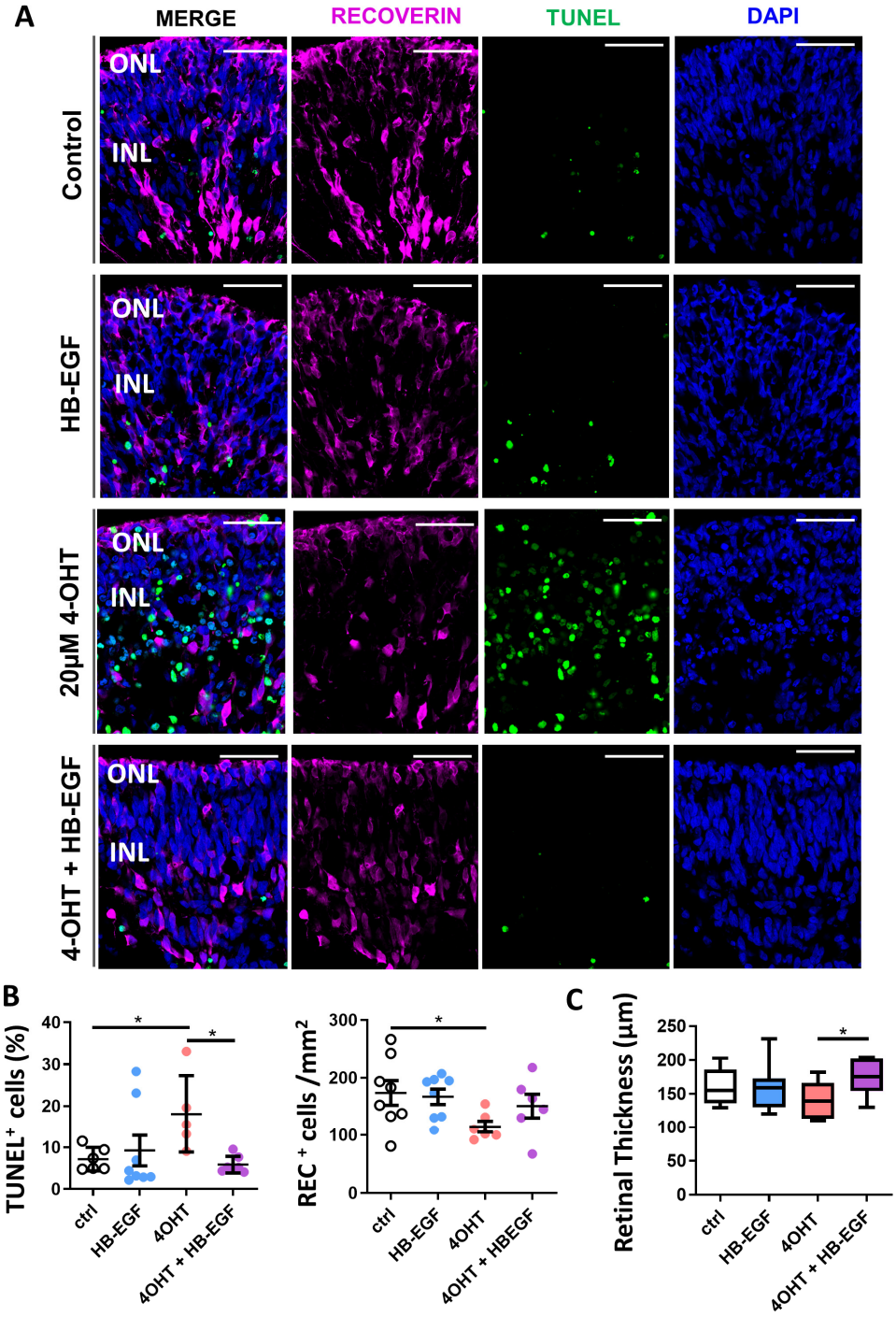

Figure 4. Examination of HB-EGF-treated organoids after 4-OHT-induced damage. Representative confocal images of retinal organoids treated with or without 4-OHT for 24 h followed by 7 days treatment

with or without HB-EGF. (**A**) Sections were stained for cell death and photoreceptor marker expression using recoverin (red) and TUNEL (green) staining. Cell nuclei were detected with DAPI (blue). 40× magnification; scale 50 µm. ONL = outer nuclear layer; INL = inner nuclear layer. (**B**) Dot plots show the % of TUNEL-positive cells and proportion of recoverin-positive cells per mm^2 in treated and untreated organoids. (**C**) Box plot shows the average thickness (µm) of retinal layers in organoids 7 days post treatment. $n = 3$. * $p < 0.05$. Student's t test. One-way ANOVA.

3.5. Müller Glial Cell Responses to 4-OHT and HB-EGF Incubation over 7 Days

Müller cell responses to HB-EGF were also examined using immunofluorescence staining. Representative fluorescence confocal images show characteristic vimentin staining with regular Muller glia processes in untreated organoids or those exposed to HB-EGF with or without 4-OHT induced damage (Figure 5A). As previously shown, retinal organoids treated with 20 µM 4-OHT for 24 h and then incubated in unconditioned medium without HB-EGF resulted in irregular and disrupted Müller cell processes as shown using vimentin staining (Figure 5A, green). Ki67-positive cells (magenta) were observed scattered throughout the width of the retinal organoid in untreated controls and those exposed to HB-EGF only or 4-OHT only (Figure 5A). In contrast, Ki67-positive cells are located in the outer retinal layers in organoids treated with 4-OHT followed by HB-EGF for 7 days (Figure 5A). Although a proportion of these cells were observed to co-localize with VSX2, the Ki67-postive cells are located in the photoreceptor layer (Figure 5A). We previously observed no changes in the number of Ki67-positive cells after 24 h, 3 days, or 7 days incubation with 20 µM 4-OHT, as shown in Figure 3. However, when examining Ki67-positive cells after 7 days following an initial 24 h 4-OHT insult, the number of Ki67-positive cells per mm^2 significantly decreased after treatment with 4-OHT alone (Figure 5B) and showed a significant increase after the addition of HB-EGF to 4-OHT damage organoids (Figure 5B). Although there was no difference in the number of VSX2-positive cells among all conditions, the number of cells positive for both Ki67 and VSX2 significantly increased after the addition of HB-EGF to the 4-OHT-damaged organoids as compared to those treated with 4-OHT alone (Figure 5B).

Further examination of the Müller glia markers vimentin and nestin showed double positive staining, with characteristic Müller glial cell like morphology as demonstrated by processes extending the width of the retinal organoid from the inner to the outer retinal layers (Figure 5C). There were no observable changes in the distribution and morphology of these cells between control organoids and those treated with HB-EGF alone or those treated with 4-OHT and HB-EGF after 7 days (Figure 5C). As shown previously, SOX2-positive cell nuclei were observed in the inner retinal organoid layers, and there was no significant difference in the number of SOX2-positive cells per mm^2 across all conditions tested (Figure 5C,D). We further examined the fluorescence intensity of nestin and vimentin in the retinal organoid cultures. In organoids treated with 4-OHT followed by unconditioned medium for 7 days, analysis showed that the fluorescence intensity was slightly reduced as compared to control organoids, but the result was not statistically significant. However, a significant increase in nestin fluorescence intensity was seen after the addition of HB-EGF for 7 days to 4-OHT-damaged organoids as compared with 4-OHT-treated organoids (Figure 5D). Similarly, measurement of the fluorescence intensity of vimentin showed a significant reduction in organoids treated with 4-OHT alone as compared to controls or those treated with HB-EGF alone, and a significant increase in intensity was observed after the addition of HB-EGF to 4-OHT-damaged organoids (Figure 5D).

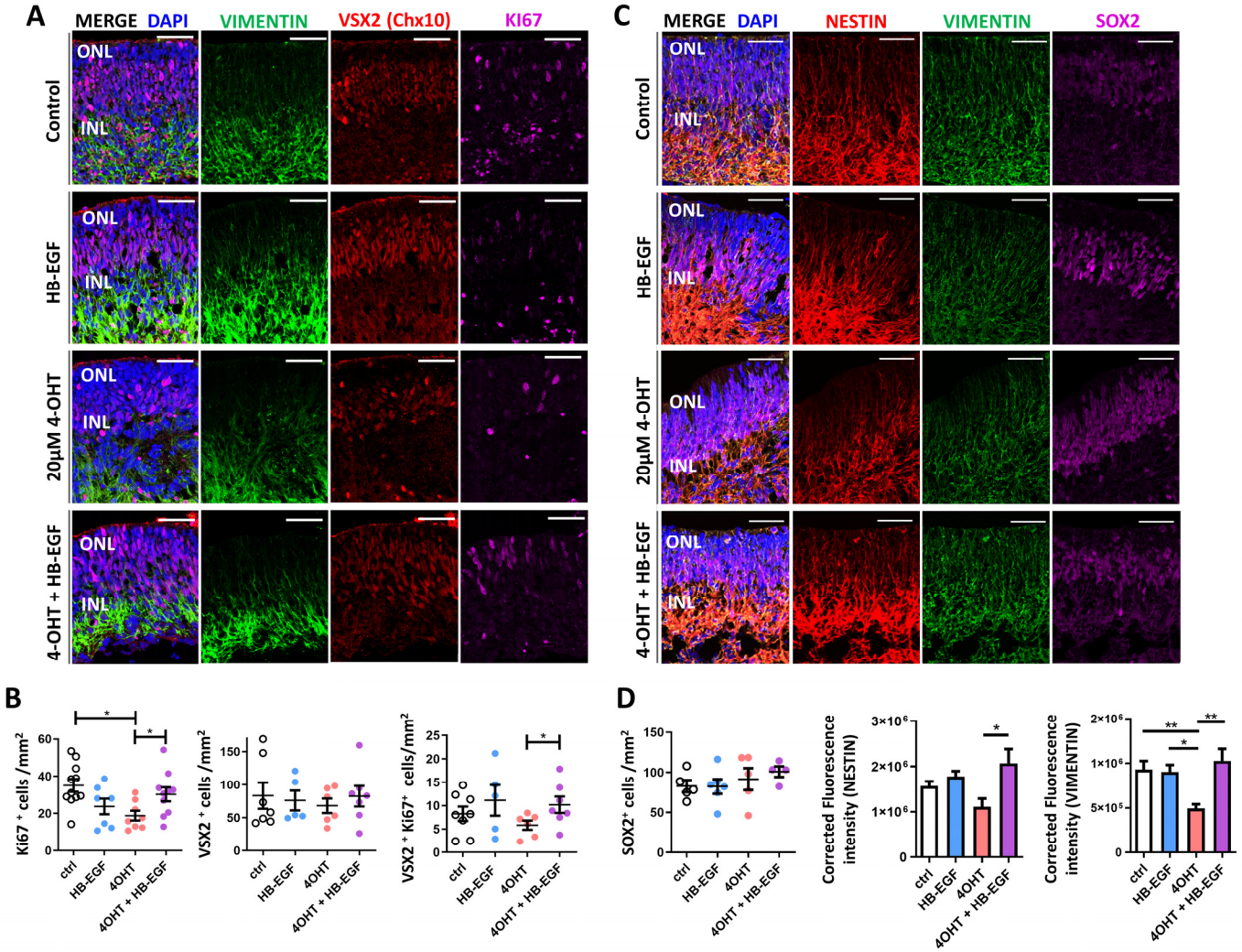

Figure 5. Examination of Müller glia by immunofluorescence in organoids treated with 4-OHT followed by HB-EGF. Representative confocal images of retinal organoids treated with or without 4-OHT for 24 h followed by 7 days treatment with or without HB-EGF. Sections were stained for (**A**) vimentin (green), Ki67 (magenta), and VSX2 (red). (**C**) Müller cell responses based on positive staining for vimentin (green), Nestin (red), and SOX2 (magenta). Cell nuclei were detected with DAPI (blue). 40× magnification; scale 50 µm. ONL = outer nuclear layer; INL = inner nuclear layer. (**B**) Dot plots show the number of Ki67, VSX2, or double positive cells per mm^2 in retinal organoids with or without 4-OHT (20 µM) and/or HB-EGF treatment as compared to those without treatment (control) after 7 days. (**D**) Dot plot shows the number of SOX2-postive cells per mm^2 after treatments, and the intensity of nestin or vimentin fluorescence staining was obtained from confocal images using ImageJ analysis. * $p < 0.05$, ** $p < 0.01$; $n = 3$. Student's t test; One-way ANOVA.

3.6. Gene Expression Analysis of Downstream Targets of HB-EGF

To investigate changes observed in histological sections of retinal organoids treated with HB-EGF, we assessed gene expression changes of known downstream targets of HB-EGF signaling (Figure 6). We examined the expression of PAX6, a downstream target of HB-EGF signaling, and NOTCH1, which is known to be reactivated during zebrafish retina regeneration. The results indicated that compared to controls, organoids treated with HB-EGF alone or 4-OHT alone showed minimal differences in PAX6 expression levels, but organoids treated with 20 µM 4-OHT followed by HB-EGF showed an increase in PAX6 expression after 7 days (Figure 6). Similarly, NOTCH1 expression showed a small log2-fold decrease in organoids treated with HB-EGF alone or 4-OHT alone, but increased expression

was observed in those treated with 4-OHT followed by HB-EGF as compared to controls after 7 days (Figure 6).

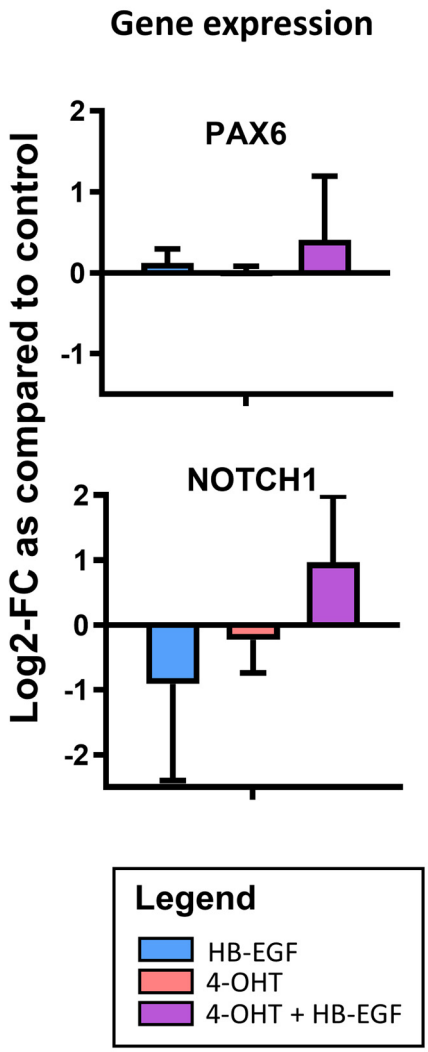

Figure 6. Gene expression analysis of organoids treated with 4-OHT followed by HB-EGF. Graphs show the relative log2-fold change (FC) in expression of the HB-EGF pathway-related genes PAX6 and NOTCH1 in organoids treated with HB-EGF alone, 4-OHT alone, or 4-OHT and HB-EGF after 7 days as compared to untreated control organoids.

4. Discussion

In the current study, we used human ESC-derived retinal organoids to examine photoreceptor and Müller cell responses in an in vitro model of retinal degeneration caused by 4-OHT, and we also sought to determine whether HB-EGF has any regenerative effect on these cells within organoids in vitro. It was found that the organized structure of retinal organoids is highly disrupted after 20 µM 4-OHT treatment, resulting in a marked reduction of photoreceptor type cells and an increase in the number of apoptotic cells. In addition, after 4-OHT treatment, subsequent treatment with HB-EGF appears to stimulate cell proliferation and leads to a reduction in the number of cells undergoing apoptosis. This may suggest that the damage induced to the retinal organoids increases the responsiveness to HB-EGF signaling and warrants further investigations.

Previous studies have shown the effect of 4-OHT on the induction of photoreceptor damage in the rodent retina as well as in mouse iPSC-derived retinal organoids [19,20]. We utilized these models to assess the effectiveness of 4-OHT on photoreceptor degeneration in human ESC retinal organoids. Currently, it is challenging to study mechanisms in normal

human donors or patients due to the difficulty in accessing fresh ex vivo donor tissue and its associated rapid decay. The use of human stem cell-derived retinal organoids could therefore constitute a suitable alternative that avoids issues such as the lack of accessibility and tissue decay as they can easily be maintained in vitro. Alternative disease models are being developed such as those using patient-derived iPSCs to grow retinal organoids with degenerative features [22–24]. These models, however, require extensive resources and expertise. In addition, the organoids generated present phenotypes for a specific genetic mutation; thus, these models do not account for all cases of retinal degeneration. The benefits of using the model presented in this study include the ease at which it can be adapted, providing a generic model with which to study mechanisms of photoreceptor degeneration that could be applied to multiple retinal degenerative diseases. Furthermore, such models reduce the need for animal experimentation while providing a more accurate representation of human retina to study mechanisms of retinal degeneration and the development of novel therapies.

Although we present a method to induce retinal degeneration in human PSC-derived retinal organoids, there are still limitations to consider when using this model. It is widely known that organoids can vary considerably in terms of shape and size, and some differences have been reported in the rate of development [25]. It is also important to consider that these organoids lack a vasculature as well as immune cells [26], which may impact studies focusing on retinal damage or repair in vivo. Additionally, functional photoreceptors do not appear to form until the late stages of differentiation ($\geq$70 days); therefore, these studies must take place over lengthy timescales. Limitations aside, this model may still provide advantages as alternatives for studying mechanisms in humans that require the use of ex vivo human donor tissue.

In the current study, we show a disruption in the number of recoverin-positive photoreceptors after the addition of 4-OHT; however, we need to consider that other neural retinal cells might be affected by 4-OHT within the retinal organoid. This was not under the remit of the current study; however, it may be important to consider in future studies. We did, however, examine the responses of Müller glia after 4-OHT-induced photoreceptor damage to human ESC-derived retinal organoids. In the current model, we observed marginal gliosis-like responses in resident Müller cells as indicated by disrupted Müller cell processes and increases in GFAP immunostaining and gene expression after treatment with 4-OHT. The lack of a robust Müller glia-like gliotic response in this model warrants further investigations but may reflect the differences in the physiological characteristics of in vitro retinal organoids as compared to in vivo tissue. In normal mammalian retina, reactive gliosis arises through complex interactions, which may include local inflammatory and immune responses, and the recruitment of microglia [27,28]; however, it has not been possible to replicate these processes in vitro within retinal organoids [29], which may account for the limited expression of GFAP in Müller glia observed in our study. However, some evidence for reactive gliosis has previously been reported in retinal [30] and cerebral [31] organoids, and these mechanisms involved warrant further studies.

Our results showed that HB-EGF stimulated cell proliferation within ESC-derived retinal organoids, but only upon the induction of 4-OHT-mediated damage to the retina. This is in contrast with previous reports in the zebrafish retina that showed that HB-EGF can drive Müller glia-mediated proliferation and formation of progenitors in the absence of damage [16]. However, our results are supported by similar studies conducted in the chick and mouse retina, indicating that HB-EGF stimulates Müller glia proliferation but only after damage [17] and suggesting that similar mechanisms may occur in the mammalian retina across species. Studies in zebrafish show that HB-EGF-mediated regeneration activates several signaling cascades, including EGFR/MAPK and Ascl1a/Notch; however, in the mouse retina, HB-EGF can lead to activation of MAPK, Jak/Stat, and mTOR signaling [17]. In the current study, we show a transient upregulation of PAX6 and NOTCH1 after 7 days treatment with HB-EGF following 4-OHT-induced damage in retinal organoids, suggesting activation of pathways that may lead to increased cell proliferation. This is supported

by our findings that show an increase in the number of Ki67-positive cells of which a high proportion are positive for the Muller marker and progenitor marker VSX2 after the addition of HB-EGF to organoids damaged by 4-OHT. Furthermore, we observed a trend that the addition of HB-EGF to control organoids resulted in a small decrease in Ki67-positive cells after 7 days, suggesting that the actions of HB-EGF occur only after damage is initiated. We currently do not know why HB-EGF may result in a reduction in the number of Ki67-positive cells. However, as we are capturing only one time point in the analysis, it may be suggested that we are missing a pivotal point that may show more differences in proliferative cells, and this would be interesting to explore in future experiments. It is also worth noting that previous studies have used a combination of HB-EGF and TNFα to induce pathological damage in mouse organoids derived from stem cells that encompasses both gliosis and proliferation [32]. It is clear therefore that there are complex mechanisms to explore with regards to investigating endogenous regeneration of the retina by Müller glia. These studies also highlight the differences between HB-EGF mediated proliferation and TNF-induced regeneration in the regeneration of the zebrafish retina and mechanisms within the mammalian retina that usually lead to gliosis and consequent detrimental effects.

We also may need to consider that any addition of chemicals or growth factors (e.g., 4-OHT, HB-EGF) may predominantly penetrate the outer layers of the retinal organoid and may primarily affect the outer layers of the cells. However, evidence of these factors diffusing to the inner layers is also indicated in our current study, as suggested by the disruption of the typically organized Müller glia structure after the addition of 4-OHT for up to 7 days. Although HB-EGF did not have any visible regenerative effect on photoreceptor cells, we observed increased proliferation and a reduction of cells undergoing apoptosis, suggesting that HB-EGF may be beneficial to the retinal organoid. The current study had only 7-day follow-up after HB-EGF stimulation, and this period may be too short to detect any potential differentiation that may occur. It is also possible that, as seen in zebrafish, the proliferation of Müller glia may give rise to progenitors over a longer duration. It is also worth noting that other factors may be required to potentiate this effect and thus merits further studies.

The developmental stages of the retinal organoids is also important to consider with regard to our results. In the current study, we have presented data on 70- to 90-day-old human stem cell-derived 3D retinal organoids, where photoreceptors expressing recoverin are known have robust expression [22]. However, it is well established that the inner retinal layers are first to develop, and photoreceptors presenting more mature features, such as outer segments, are slow and may take more than 150 days [22,33]. This is also true for retinal organoids derived from mouse ESCs [31]. Before undertaking such long-term studies, we chose to investigate the effects of HB-EGF at earlier maturation stages to reduce cost and time restraints. As our results have presented preliminary evidence for Muller glia reactivity and the protective effects of HB-EGF, we hope that future studies will build upon these findings by the investigation of later stage organoids with mature photoreceptors and robust lamination.

5. Conclusions

In conclusion, our results indicate that ESC-derived retinal organoids can be used as 3D models of retinal degeneration in vitro due to their responses to chemical-induced damage and receptivity for the study of regenerative factors that may be potentially used for developing new retinal therapies. In addition, our results demonstrated preliminary evidence for Muller glia reactivity and the protective effects of HB-EGF after acute damage to the retinal organoid. However, further studies are needed to identify mechanisms that may induce Müller cell-mediated regeneration, which would help in the future development of endogenous regenerative therapies for retinal disease.

Supplementary Materials: The following supporting information can be downloaded at: https://www.mdpi.com/article/10.3390/organoids3030010/s1, Table S1: List of primary antibodies; Table S2: Human qPCR primers for SYBR green assays.

Author Contributions: K.E. devised and planned the experimental design under guidance of G.A.L. M.M., N.A.S., M.N.H.T. and K.E. conducted the experiments and analyzed the data. K.E. wrote the manuscript. All authors contributed to critical evaluation for intellectual content. All authors have read and agreed to the published version of the manuscript.

Funding: This work was funded by a Springboard award provided by Moorfields Eye Charity (GR001204) and supported by Santen Pharmaceutical Co., Ltd.

Institutional Review Board Statement: Not applicable.

Informed Consent Statement: Not applicable.

Data Availability Statement: The data underlying this article are available in the article and its online Supplementary Material. If further details are required, this information may be shared upon reasonable request to the corresponding author.

Acknowledgments: This work was funded by a Springboard award provided by Moorfields Eye Charity and supported by the NIHR Biomedical Research Centre at Moorfields Eye Hospital; UCL Institute of Ophthalmology, London, UK; and Santen Pharmaceutical Co., Ltd.

Conflicts of Interest: The authors declare that the research was partly conducted with support from Santen Pharmaceuticals and that KE and NAS are employees of Santen, which could be construed as potential conflicts of interest.

References

1. Becker, S.; Singhal, S.; Jones, M.F.; Eastlake, K.; Cottrill, P.B.; Jayaram, H.; Limb, G.A. Acquisition of RGC phenotype in human Muller glia with stem cell characteristics is accompanied by upregulation of functional nicotinic acetylcholine receptors. *Mol. Vis.* **2013**, *19*, 1925–1936. [PubMed]
2. Eastlake, K.; Wang, W.; Jayaram, H.; Murray-Dunning, C.; Carr, A.J.F.; Ramsden, C.M.; Vugler, A.; Gore, K.; Clemo, N.; Stewart, M.; et al. Phenotypic and Functional Characterization of Müller Glia Isolated from Induced Pluripotent Stem Cell-Derived Retinal Organoids: Improvement of Retinal Ganglion Cell Function upon Transplantation. *Stem Cells Transl. Med.* **2019**, *8*, 775–784. [CrossRef] [PubMed]
3. Bringmann, A.; Pannicke, T.; Grosche, J.; Francke, M.; Wiedemann, P.; Skatchkov, S.N.; Osborne, N.N.; Reichenbach, A. Müller cells in the healthy and diseased retina. *Prog. Retin. Eye Res.* **2006**, *25*, 397–424. [CrossRef] [PubMed]
4. Yurco, P.; Cameron, D.A. Responses of Müller glia to retinal injury in adult zebrafish. *Vision. Res.* **2005**, *45*, 991–1002. [CrossRef] [PubMed]
5. Langhe, R.; Chesneau, A.; Colozza, G.; Hidalgo, M.; Ail, D.; Locker, M.; Perron, M. Müller glial cell reactivation in Xenopus models of retinal degeneration. *Glia* **2017**, *65*, 1333–1349. [CrossRef] [PubMed]
6. Fischer, A.J.; Reh, T.A. Muller glia are a potential source of neural regeneration in the postnatal chicken retina. *Nat. Neurosci.* **2001**, *4*, 247–252. [CrossRef] [PubMed]
7. Karl, M.O.; Hayes, S.; Nelson, B.R.; Tan, K.; Buckingham, B.; Reh, T.A. Stimulation of neural regeneration in the mouse retina. *Proc. Natl. Acad. Sci. USA* **2008**, *105*, 19508–19513. [CrossRef]
8. Bhatia, B.; Singhal, S.; Lawrence, J.M.; Khaw, P.T.; Limb, G.A. Distribution of Müller stem cells within the neural retina: Evidence for the existence of a ciliary margin-like zone in the adult human eye. *Exp. Eye Res.* **2009**, *89*, 373–382. [CrossRef] [PubMed]
9. Lawrence, J.M.; Singhal, S.; Bhatia, B.; Keegan, D.J.; Reh, T.A.; Luthert, P.J.; Khaw, P.T.; Limb, G.A. MIO-M1 cells and similar muller glial cell lines derived from adult human retina exhibit neural stem cell characteristics. *Stem Cells* **2007**, *25*, 2033–2043. [CrossRef]
10. Singhal, S.; Bhatia, B.; Jayaram, H.; Becker, S.; Jones, M.F.; Cottrill, P.B.; Khaw, P.T.; Salt, T.E.; Limb, G.A. Human Müller glia with stem cell characteristics differentiate into retinal ganglion cell (RGC) precursors in vitro and partially restore RGC function in vivo following transplantation. *Stem Cells Transl. Med.* **2012**, *1*, 188–199. [CrossRef]
11. Eastlake, K.; Heywood, W.E.; Tracey-White, D.; Aquino, E.; Bliss, E.; Vasta, G.R.; Mills, K.; Khaw, P.T.; Moosajee, M.; Limb, G.A. Comparison of proteomic profiles in the zebrafish retina during experimental degeneration and regeneration. *Sci. Rep.* **2017**, *7*, 44601. [CrossRef]
12. Stanchfield, M.L.; Webster, S.E.; Webster, M.K.; Linn, C.L. Involvement of HB-EGF/Ascl1/Lin28a Genes in Dedifferentiation of Adult Mammalian Müller Glia. *Front. Mol. Biosci.* **2020**, *7*, 200. [CrossRef] [PubMed]
13. Elsaeidi, F.; Macpherson, P.; Mills, E.A.; Jui, J.; Flannery, J.G.; Goldman, D. Notch Suppression Collaborates with Ascl1 and Lin28 to Unleash a Regenerative Response in Fish Retina, But Not in Mice. *J. Neurosci.* **2018**, *38*, 2246–2261. [CrossRef]

14. Gorsuch, R.A.; Lahne, M.; Yarka, C.E.; Petravick, M.E.; Li, J.; Hyde, D.R. Sox2 regulates Muller glia reprogramming and proliferation in the regenerating zebrafish retina via Lin28 and Ascl1a. *Exp. Eye Res.* **2017**, *161*, 174–192. [CrossRef] [PubMed]
15. Shin, S.Y.; Yokoyama, T.; Takenouchi, T.; Munekata, E. The chemical synthesis and binding affinity to the EGF receptor of the EGF-like domain of heparin-binding EGF-like growth factor (HB-EGF). *J. Pept. Sci.* **2003**, *9*, 244–250. [CrossRef]
16. Wan, J.; Ramachandran, R.; Goldman, D. HB-EGF is necessary and sufficient for Müller glia dedifferentiation and retina regeneration. *Dev. Cell* **2012**, *22*, 334–347. [CrossRef] [PubMed]
17. Todd, L.; Volkov, L.I.; Zelinka, C.; Squires, N.; Fischer, A.J. Heparin-binding EGF-like growth factor (HB-EGF) stimulates the proliferation of Müller glia-derived progenitor cells in avian and murine retinas. *Mol. Cell Neurosci.* **2015**, *69*, 54–64. [CrossRef]
18. Hollborn, M.; Tenckhoff, S.; Jahn, K.; Iandiev, I.; Biedermann, B.; Schnurrbusch, U.E.; Limb, G.A.; Reichenbach, A.; Wolf, S.; Wiedemann, P.; et al. Changes in retinal gene expression in proliferative vitreoretinopathy: Glial cell expression of HB-EGF. *Mol. Vis.* **2005**, *11*, 397–413.
19. Onishi, A.; Peng, G.-H.; Poth, E.M.; Lee, D.A.; Chen, J.; Alexis, U.; de Melo, J.; Chen, S.; Blackshaw, S. The orphan nuclear hormone receptor ERRbeta controls rod photoreceptor survival. *Proc. Natl. Acad. Sci. USA* **2010**, *107*, 11579–11584. [CrossRef]
20. Ito, S.I.; Onishi, A.; Takahashi, M. Chemically-induced photoreceptor degeneration and protection in mouse iPSC-derived three-dimensional retinal organoids. *Stem Cell Res.* **2017**, *24*, 94–101. [CrossRef]
21. De Sousa, P.; Tye, B.; Bruce, K.; Dand, P.; Russell, G.; Collins, D.; Greenshields, A.; McDonald, K.; Bradburn, H.; Canham, M.; et al. Derivation of the clinical grade human embryonic stem cell line RCe013-A (RC-9). *Stem Cell Res.* **2016**, *17*, 36–41. [CrossRef] [PubMed]
22. Nakano, T.; Ando, S.; Takata, N.; Kawada, M.; Muguruma, K.; Sekiguchi, K.; Saito, K.; Yonemura, S.; Eiraku, M.; Sasai, Y. Self-formation of optic cups and storable stratified neural retina from human ESCs. *Cell Stem Cell* **2012**, *10*, 771–785. [CrossRef] [PubMed]
23. Lane, A.; Jovanovic, K.; Shortall, C.; Ottaviani, D.; Panes, A.B.; Schwarz, N.; Guarascio, R.; Hayes, M.J.; Palfi, A.; Chadderton, N.; et al. Modeling and Rescue of RP2 Retinitis Pigmentosa Using iPSC-Derived Retinal Organoids. *Stem Cell Rep.* **2020**, *15*, 67–79. [CrossRef] [PubMed]
24. Zhang, X.; Zhang, D.; Thompson, J.A.; Chen, S.; Huang, Z.; Jennings, L.; McLaren, T.L.; Lamey, T.M.; De Roach, J.N.; Chen, F.K.; et al. Gene correction of the CLN3 c.175G>A variant in patient-derived induced pluripotent stem cells prevents pathological changes in retinal organoids. *Mol. Genet. Genom. Med.* **2021**, *9*, e1601. [CrossRef] [PubMed]
25. Lukovic, D.; Castro, A.A.; Kaya, K.D.; Munezero, D.; Gieser, L.; Davó-Martínez, C.; Corton, M.; Cuenca, N.; Swaroop, A.; Ramamurthy, V.; et al. Retinal Organoids derived from hiPSCs of an AIPL1-LCA Patient Maintain Cytoarchitecture despite Reduced levels of Mutant AIPL1. *Sci. Rep.* **2020**, *10*, 5426. [CrossRef] [PubMed]
26. Capowski, E.E.; Samimi, K.; Mayerl, S.J.; Phillips, M.J.; Pinilla, I.; Howden, S.E.; Saha, J.; Jansen, A.D.; Edwards, K.L.; Jager, L.D.; et al. Reproducibility and staging of 3D human retinal organoids across multiple pluripotent stem cell lines. *Development* **2019**, *146*, dev171686. [CrossRef] [PubMed]
27. Singh, R.K.; Nasonkin, I.O. Limitations and Promise of Retinal Tissue from Human Pluripotent Stem Cells for Developing Therapies of Blindness. *Front. Cell Neurosci.* **2020**, *14*, 179. [CrossRef] [PubMed]
28. Reichenbach, A.; Bringmann, A. *Muller Cells in the Healthy and Diseased Retina*, 1st ed.; Springer: Berlin/Heidelberg, Germany, 2010.
29. Bringmann, A.; Wiedemann, P. Müller Glial Cells in Retinal Disease. *Ophthalmologica* **2012**, *227*, 1–19. [CrossRef] [PubMed]
30. Fathi, M.; Ross, C.T.; Hosseinzadeh, Z. Functional 3-Dimensional Retinal Organoids: Technological Progress and Existing Challenges. *Front. Neurosci.* **2021**, *15*, 668857. [CrossRef]
31. Völkner, M.; Kurth, T.; Schor, J.; Ebner, L.J.A.; Bardtke, L.; Kavak, C.; Hackermüller, J.; Karl, M.O. Mouse Retinal Organoid Growth and Maintenance in Longer-Term Culture. *Front. Cell Dev. Biol.* **2021**, *9*, 645704. [CrossRef]
32. Qiao, H.; Zhao, W.; Guo, M.; Zhu, L.; Chen, T.; Wang, J.; Xu, X.; Zhang, Z.; Wu, Y.; Chen, P. Cerebral Organoids for Modeling of HSV-1-Induced-Amyloid β Associated Neuropathology and Phenotypic Rescue. *Int. J. Mol. Sci.* **2022**, *23*, 5981. [CrossRef]
33. Wahlin, K.J.; Maruotti, J.A.; Sripathi, S.R.; Ball, J.; Angueyra, J.M.; Kim, C.; Grebe, R.; Li, W.; Jones, B.W.; Zack, D.J. Photoreceptor Outer Segment-like Structures in Long Term 3D retinas from human pluripotent stem cells. *Sci. Rep.* **2017**, *7*, 766. [CrossRef]